


 Cite this: *J. Anal. At. Spectrom.*, 2025, **40**, 1726

# The influence of cone orifice diameter on ion transmission in solution and laser ablation ICP-MS†

 Claire A. Richards, Matthew A. Turner and Amy J. Managh \*

Optimal sampler and skimmer cone orifice diameter has been well developed for solution based inductively coupled plasma-mass spectrometry (ICP-MS) but is not fully understood for modern laser ablation (LA) systems. This research investigates the impact of various cone orifice sets and the effect they have on ICP-MS sensitivity using solution mode and whilst using a low-dispersion LA system. A wide range of elements between the masses  ${}^7\text{Li}$  and  ${}^{238}\text{U}$  and their oxides have been measured *via* solution nebulisation as well as NIST 610 glass reference material and multi-elemental gelatine microdroplets *via* laser ablation. For multi-elemental micro droplets, 7 out of 11 elements analysed showed a statistically significant increase in sensitivity when a reduction of cone orifice size of 0.1 mm was used, compared to the standard cone orifice size. Similarly, for the ablation of NIST 610, 7 out of 11 elements displayed a statistically higher sensitivity with a 0.1 mm reduced orifice size. This analysis has confirmed suitability of standard cone sets for nebulisation of homogeneous solutions whilst suggesting a slight reduction in cone orifice diameter improves ion transmission through the cones towards the mass spectrometer by up to 272% (NIST 610) or 124% (multi-elemental droplets) for LA-ICP-MS.

 Received 6th February 2025  
Accepted 21st May 2025

DOI: 10.1039/d5ja00046g

[rsc.li/jaas](https://rsc.li/jaas)

## Introduction

Inductively coupled plasma-mass spectrometry (ICP-MS) is a widely used technique for elemental analysis, due to its ability to detect and quantify most elements in the periodic table with high sensitivity. Since its introduction in the 1980's, many aspects of the core instrumentation have evolved, including the development of more efficient sample introduction systems, changes to the ion optics, and the implementation of a wider range of mass analysers.<sup>1–6</sup> However, the mass spectrometer interface, which is one of the most inefficient regions of the ICP-MS,<sup>7</sup> has undergone relatively fewer changes during this period. The interface consists of two (or more) metallic cones, which enable a staged reduction in the pressure from the atmospheric pressure plasma to the cooler high vacuum environment of the mass spectrometer. Ions first pass through an orifice in the sampler cone, into an intermediate vacuum of a few mbar, where they experience supersonic expansion. The skimmer cone then selectively transfers the central channel of this expanded jet through its orifice towards the ion optics of the mass spectrometer. The interface region is the primary site for oxide formation,<sup>8</sup> a phenomenon that is detrimental to the analysis of many elements below  $m/z$  80. This region has therefore been the subject of a number of fundamental studies,

which have shown that modifications to the cone shapes/angles, materials and orifice sizes can have a profound impact on their performance.<sup>9–13</sup> One example is the introduction of the jet interface, which uses a larger orifice diameter coupled with higher pumping capacity to increase ion transmission.<sup>14</sup> The majority of studies have investigated the interface when operating the ICP-MS in 'wet plasma' mode, by nebulising liquid samples. However, relatively fewer work has been reported for other introduction modes such as laser ablation (LA).

Sampling of solids by laser ablation was first coupled to ICP-MS in 1985,<sup>15</sup> and its use with ICP-MS has since gained popularity across a wide range of fields such as the bio- and geosciences.<sup>16–20</sup> The nature of sample introduction by LA is fundamentally different to that produced by solution nebulisation. The dry LA aerosol is introduced in discrete packages with mass loading of  $\text{ng s}^{-1}$ , compared to  $>100 \mu\text{g s}^{-1}$  streams of solvent droplets generated by a nebuliser. LA typically also involves addition of a carrier gas to the central channel and this is commonly helium. Such fundamental differences in the introduced aerosol may affect the temperature and shape of the plasma, degree of analyte ionisation and efficiency of transport through the interface.<sup>21–23</sup> There have been comparatively fewer articles that focus on dry plasma conditions when evaluating cones. In an early study, Günther *et al.* showed that the entrainment of air can have a large impact on the signal recorded under dry plasma conditions, which can affect the signal-to-noise ratio and hence, the limits of detection.<sup>24</sup> Improved limits of detection were demonstrated when reducing the orifice of the sampler cone from 0.7 mm to 0.5 mm. The

Department of Chemistry, Loughborough University, Epinal Way, Loughborough, Leicestershire, LE11 3TU, UK. E-mail: [A.J.Managh@lboro.ac.uk](mailto:A.J.Managh@lboro.ac.uk)

† Electronic supplementary information (ESI) available. See DOI: <https://doi.org/10.1039/d5ja00046g>



study was followed up by a later investigation, which was expanded to include the skimmer cones, and again showed a reduction in oxide formation when using smaller orifice sizes.<sup>25</sup> In 2018, He *et al.*, looked at commercially available cone combinations with different geometries, observing variations in sensitivity of a factor between 1.5 and 9.7, dependent on the orifice shape.<sup>26</sup>

Since the above studies there has been significant progress in the way that laser ablated aerosols are transported into the plasma. Several developments have been introduced to reduce turbulent mixing within the ablation cells and during transport to the ICP, enabling improvements in the speed and sensitivity of analysis.<sup>27–29</sup> Some of these devices are designed to establish the central channel of the plasma independently of the LA gas flow, enabling the introduction of ablated particulate on axis with the inlet.<sup>28,30</sup> This may potentially reduce radial dispersion of the material in the plasma, improving ion transmission. As these devices are now becoming routine, it is important to assess their impacts on the mass spectrometer interface. In the present paper, the cone orifice sizes are re-investigated using a low dispersion LA system. Impacts on ion transmission, background signals and oxide formation are also compared to traditional solution-based analysis using the same cones, which to the authors knowledge, is the first comparison of this kind.

## Experimental

### Sample preparation

An in-house made 1 ppm multi-elemental standard solution containing 1 ppm Li, K, Fe, Ni, Se, Sr, Cd, Ba, Tl, Th and U was prepared from single element calibration standards from a variety of suppliers (Sigma-Aldrich and Fisher Scientific, UK, SPEX CertiPrep and Ultra Scientific, USA). For homogenous solution analysis, the multi-elemental solution was diluted to 1 ppb using 2% nitric acid prepared from ROMIL-UpA™ Ultra Purity Acid (ROMIL, UK). Ultrapure water with a resistance of 18.2 MΩ cm from an Avidity Science water purification system was used as a source of deionised water in this study.

A MD-E-3011-130 piezoelectric microdroplet dispenser system (Microdrop Technologies GmbH, Germany), fitted with an MD-K0130-20 dispenser head was used to print droplets onto a dried 10% gelatine film on a glass microscope slide, as described by Greenhalgh *et al.*<sup>31</sup> A computer-controlled *x-y* stage was used to position the slide beneath the droplet generator, enabling a grid pattern of the droplets to be printed. The resulting droplet array had an average droplet size of 141.0 μm (0.77% RSD) length by 114.8 μm (1.31% RSD) width.

### ICP-MS instrumentation

Analyses were performed using an Element XR ICP-MS (Thermo Scientific, Germany). The study was carried out using custom made nickel sampler and skimmer cones purchased from Spectron LLC, USA, with certified sampler cone orifice sizes of 1.1, 1.0 and 0.7 mm and skimmer cone orifice sizes of 0.8, 0.7, and 0.5 mm. Five combinations of these sampler and skimmer cones were studied, according to Table 1. Post analysis, the size

Table 1 Sampler and skimmer cone size combinations

Cone combination	Sampler cone orifice/mm	Skimmer cone orifice/mm	Sampler/skimmer orifice ratio
1.1 samp/0.8 skim	1.1	0.8	1.375
1.1 samp/0.5 skim	1.1	0.5	2.200
1.0 samp/0.7 skim	1.0	0.7	1.420
0.7 samp/0.8 skim	0.7	0.8	0.875
0.7 samp/0.5 skim	0.7	0.5	1.400

and structural integrity of the orifices were examined under a Keyence VHX-7100 Digital Microscope to evaluate signs of wear after a 10-day use period (ESI Fig. S1†).

For solution measurements, the ICP-MS was fitted with a quartz cyclonic spray chamber (Glass Expansion, Australia), a MicroFlow PFA Nebulizer and a 0.25 mm ID probe (both Elemental Scientific, USA). For laser ablation experiments, an NWR Image 266 nm laser ablation system (Elemental Scientific Lasers, USA) was coupled to the ICP-MS *via* a Direct Concentric Injector (DCI).

### ICP-MS analysis

An overview of operating parameters used in this experiment are summarised in Table 2. The ICP-MS was tuned for maximum uranium sensitivity whilst keeping the UO/U ratio below 1% for dry plasma analysis and below 5% for wet plasma analysis. Tuning of the *x* and *y* torch positions were re-optimised between cone sets to account for small differences when inserting the cones. However, no notable differences were observed. Whole droplets were ablated using a rastered approach, where three droplets were measured per element, for each cone combination tested. Analyses were also performed on NIST 610 glass reference material using a drilling down approach. For all samples, the measured isotopes were <sup>7</sup>Li, <sup>39</sup>K, <sup>57</sup>Fe, <sup>60</sup>Ni, <sup>78</sup>Se (solution), <sup>77</sup>Se (LA), <sup>88</sup>Sr, <sup>137</sup>Ba, <sup>137</sup>Ba<sup>16</sup>O, <sup>205</sup>Tl, <sup>232</sup>Th, <sup>232</sup>Th<sup>16</sup>O, <sup>238</sup>U, <sup>238</sup>U<sup>16</sup>O, with a single isotope measured per run.

### LA-ICP-MS data processing

Data was processed using a freeware app, the LA-ICP-MS ImageTool 1.7, which has been described previously.<sup>32</sup> Gelatine droplet data was converted into a 2D colour coded pixel image using baseline separated peaks to show the distribution of analytes across the ablated region. The data was then exported into Microsoft Excel as a csv file, where total signal recorded within each droplet was summed to give the total count per droplet. The collection of NIST 610 glass reference material data was not designed to produce an image due to the drilling down methodology used. Instead, individual peaks within a consistent time-period between 12.5 and 17.5 seconds was considered; data for the shots up to 12.5 seconds were discarded to allow for surface roughness. Data from each cone set was normalised to the standard cone set (1.1 samp/0.8 skim) for comparison. One standard deviation was calculated and used for display of error bars on figures. In this study, *t*-tests



Table 2 Experimental operating parameters

Parameter	LA-gelatine	LA-NIST 610	Solution
RF power	1070 W	1070 W	1070 W
Torch z position	−2.5 mm	−2.5 mm	−2.5 mm
Argon cooling gas flow	15.75 L min <sup>−1</sup>	15.75 L min <sup>−1</sup>	15.75 L min <sup>−1</sup>
Argon auxiliary gas flow	0.85 L min <sup>−1</sup>	0.85 L min <sup>−1</sup>	0.85 L min <sup>−1</sup>
Argon sample gas flow	0.55 L min <sup>−1</sup>	0.55 L min <sup>−1</sup>	0.94 L min <sup>−1</sup>
Helium gas flow	1.2 L min <sup>−1</sup>	1.2 L min <sup>−1</sup>	—
Laser fluence	13.0 J cm <sup>−2</sup>	13.8 J cm <sup>−2</sup>	—
Repetition frequency	5 Hz	5 Hz	—
Spot size	10 μm	25 μm	—
Scan speed	50 μm s <sup>−1</sup>	—	—

were carried out using an alpha value of 0.05 as a threshold for statistically significant differences.

## Results and discussion

### Sensitivity of cone sets in wet plasma mode

The initial part of the experiment investigated a reduction of the cone orifice size, whilst keeping the ratio between the sampler and skimmer orifices approximately constant. The normalised signal intensity of these compared to the standard set is shown in Fig. 1. In this study, 'standard' cone set refers to a sampler cone orifice diameter of 1.1 mm and skimmer cone orifice of 0.8 mm and is the typical set of cones recommended for the instrument. In accordance with previous literature,<sup>9</sup> the standard cone set produced the highest ion transmission.

An almost complete drop off in signal intensity is seen when the smallest cone set is used, with a statistically significant rise

in oxide formation for uranium and thorium. A slight reduction in the size of the standard orifices by 0.1 mm results in a less pronounced drop off in signal intensity, whereby the signal is reduced by between 78.8% and 35.6% (relative to the standard cone set) over the mass range studied. It is clear from the data in Fig. 1 that moving to smaller orifice sizes results in a more pronounced mass bias across the mass range studied. This is due to enhanced space charge effects in the interface region of the mass spectrometer when using a smaller diameter inlet.

The second investigation studied combinations from different cone sets to evaluate whether changing the ratios away from the manufacturer recommended specification influences the signal (see ESI Fig. S2 and S3†). In each case, one of the cones was kept to the manufacturer recommended size and the other was changed to the most extreme low condition (see Table 1). Both combinations studied showed a statistically significantly lower sensitivity than the standard cone set (1.1

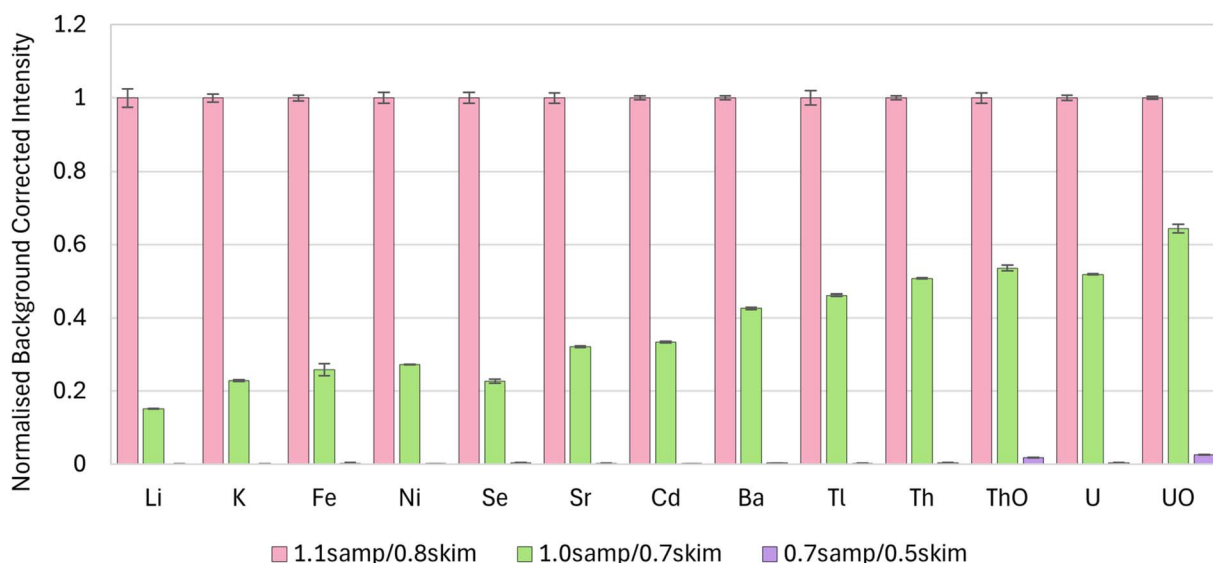


Fig. 1 Normalised signal intensity plot for analysis of a 1 ppb solution using wet plasma ICP-MS. Comparison of the standard cone set (1.1 mm sampler/0.8 mm skimmer) to cone sets which reduced the orifice diameters whilst maintaining the sampler to skimmer orifice ratio (1.0 mm sampler/0.7 mm skimmer, green and 0.7 mm sampler/0.5 mm skimmer, purple). Error bars represent  $\pm 1$  standard deviation for mean signal intensity where  $n = 3$ , normalised to standard cone orifice set. Elements arranged in increasing mass-to-charge from left to right. All differences in intensity between standard cone set and other sets are statistically significant ( $t$ -test). See ESI Fig. S2 and S3† for comparison of all orifice sizes studied.



samp/0.8 skim) across all elements and oxides investigated. Therefore, in terms of signal intensity there is no apparent benefit from moving away from the manufacturer recommended ratios for solution experiments. However, it was noted that in terms of signal-to-noise ratio, the set that used the standard sampler and the smallest skimmer (1.1 samp/0.5 skim) provided the highest signal-to-noise ratio for masses of Sr and above (see ESI Fig. S4†). It would be unlikely that this cone combination would be used in practice due to the significantly lower sensitivity observed. Additionally, cones manufactured with smaller orifices are more fragile and the orifice tip shape is prone to wear (ESI Fig. S1†), suggesting that this cone size or smaller is not practical for extensive use. This problem was not observed with the larger cone sizes.

### Sensitivity of cone sets in dry plasma mode

**Ablation of multi-elemental droplets (soft particles).** The same combination of cones used in solution mode were also used to measure signal intensity from laser ablated multi-elemental droplets and this data is represented in Fig. 2. Mass bias due to the space charge effect shown by solution data is less prevalent within this data set, although, as with wet plasma conditions, it is evident that using the smallest set of cones (0.7 samp/0.5 skim) results in a statistically significant drop off in sensitivity. The pronounced drop off in signal intensity when reducing both orifice sizes by 0.1 mm was not observed in dry plasma mode.

For all elements, excluding Se, the background corrected signal intensity was either statistically equivalent or significantly higher for the 0.1 mm reduced cone set. Of the elements measured in this study, Se had the highest first ionisation

potential (see ESI Table S1†). Across all the elements studied, the average increase was 43% (see ESI Table S2†). The small reduction in the sampler orifice size also produced an improvement in signal-to-noise ratio for 5 out of the 11 elements studied (ESI Fig. S6†). However, in dry plasma mode background signals were generally very low (<100 counts per pixel for all elements beyond Ni), thus the trend in signal-to-noise ratio between cone sets was inconsequential.

The authors hypothesise that the improved ion transmission for some elements is due to lower vacuum readings achieved which extracted material more efficiently through the cones. Reducing the cone set beyond this point did not produce any further improvements in ion transmission.

Changing the ratios between the sampler and skimmer cones did not produce an improvement over the standard cone sets. Changing the sampler from 1.1 mm to 0.7 mm, whilst keeping the skimmer cone at the manufacturer recommended size, resulted in an average signal reduction of 32% across the mass range, but provided a higher signal-to-noise ratio than the standard sampler for 7 out of 11 elements (see ESI Fig. S5 and S6†). Changing the skimmer from 0.8 to 0.5 mm, whilst keeping the sampler cone at the manufacturer recommended size, resulted in large signal reduction of 79%. There was no improvement in signal-to-noise ratio when using this cone combination.

Thorium and uranium oxide production was also investigated. For uranium analysis in dry plasma mode, all four of the custom cone sets produced a % oxide ratio that was statistically lower than for the standard set. When comparing thorium oxide ratio in dry plasma mode, all cone sets produced a statistically equivalent ratio, except the 0.7 samp/0.8 skim set, which was significantly smaller.

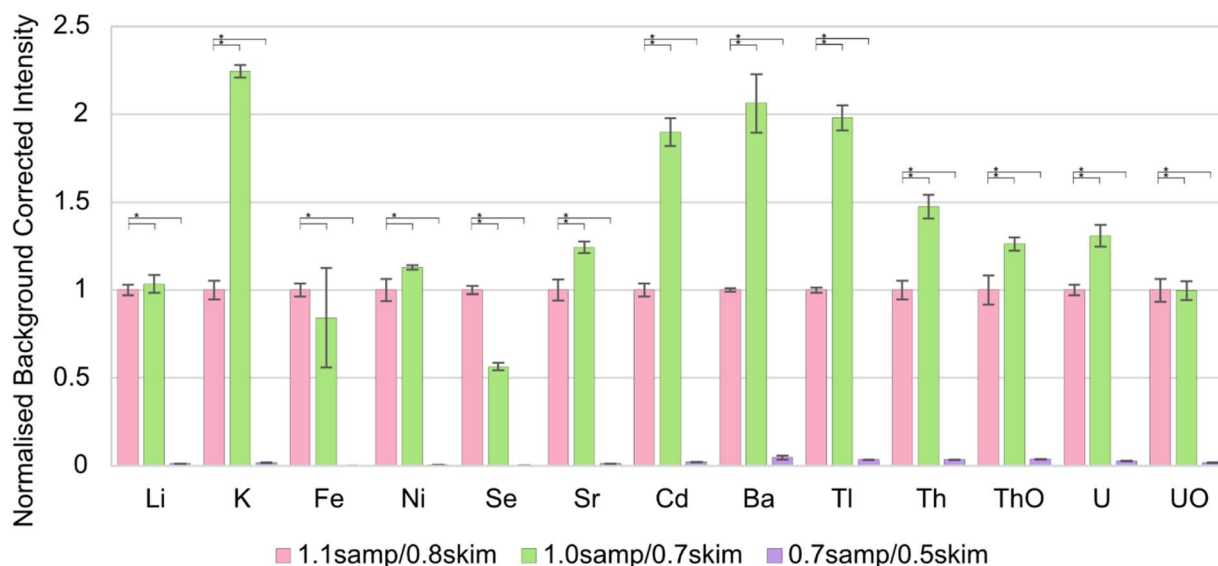


Fig. 2 Normalised background subtracted signal intensity plot for comparison of two cone sets to the standard cone set (1.1 mm sampler/0.8 mm skimmer) for dry plasma experimental setup using LA-ICP-MS analysis of gelatine spots. Error bars represent  $\pm 1$  standard deviation for mean signal intensity where  $n = 3$ , normalised to standard cone orifice set. Elements arranged in increasing mass-to-charge ratio from left to right. Horizontal lines with asterisks represent a statistically significant difference between the connected data bars at 95% confidence ( $t$ -test). See ESI Fig. S5† for comparison of all orifice sizes studied.



An example of the ablated multi-elemental droplets for each element and oxide is displayed in Fig. 3. A significant amount of leaching into the gelatine is displayed by thallium, and to

a lesser extent, lithium. The coffee-ring effect is shown by all ablated droplets where a higher signal intensity is seen in the centre of the droplet. This effect has not impacted the results of

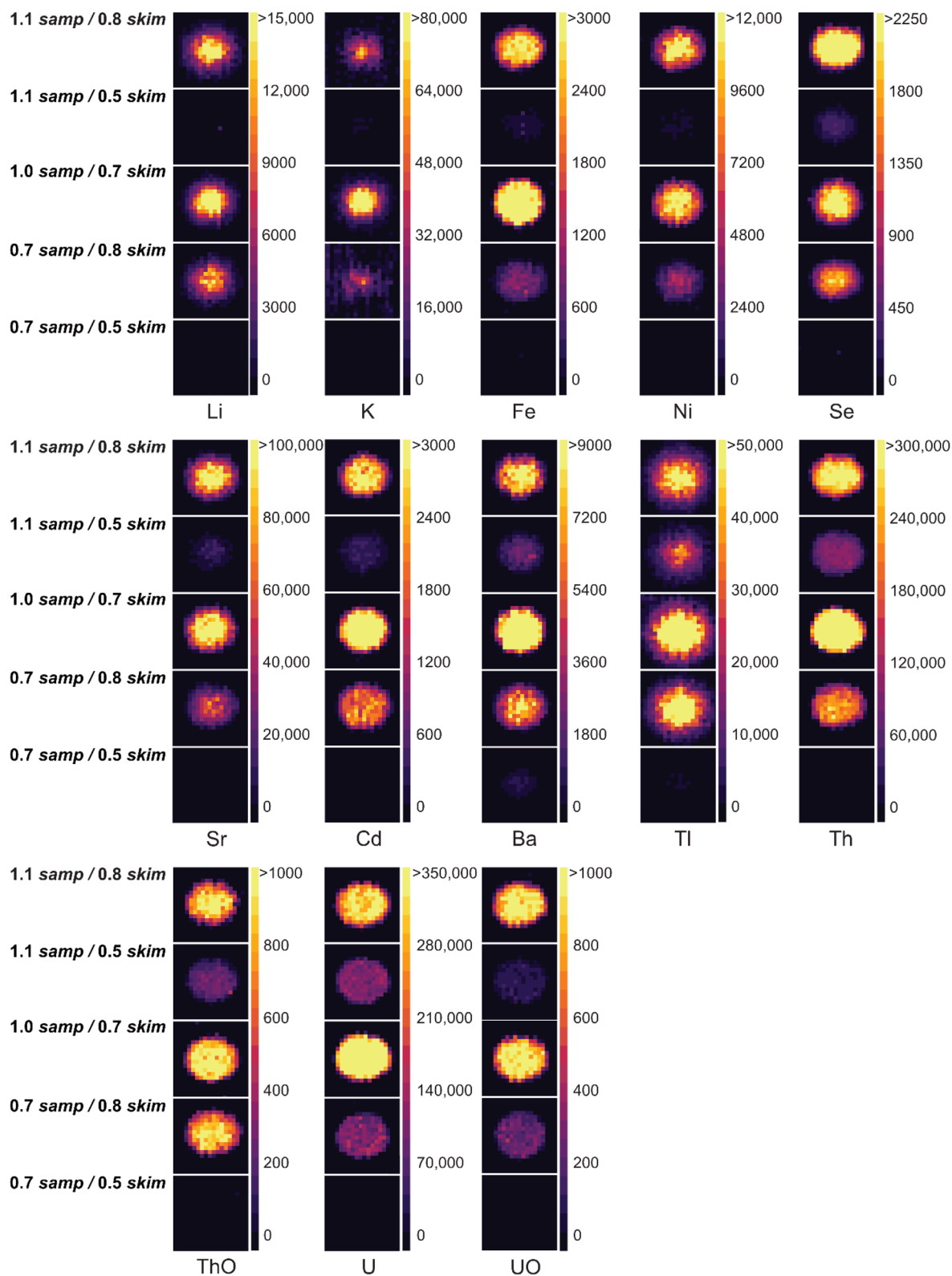


Fig. 3 Multi-elemental droplets analysed by LA-ICP-MS with different cone sets. The colour scale on the right-hand side of each plot depicts background corrected signal intensity in counts. Each window represents a  $190 \mu\text{m} \times 190 \mu\text{m}$  ablated area.



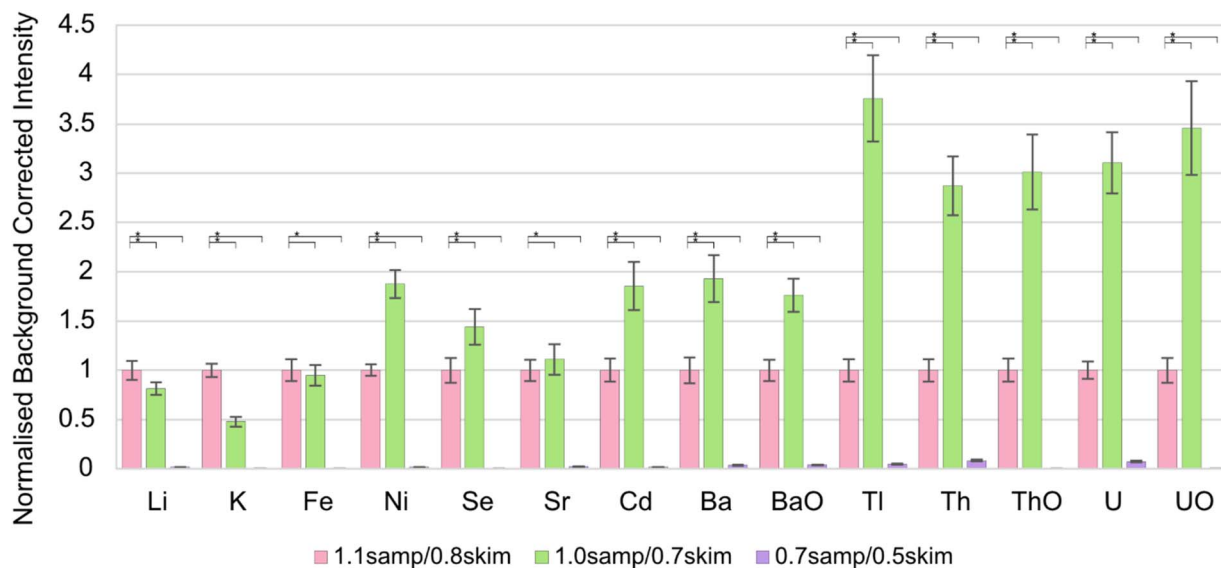


Fig. 4 Normalised background subtracted signal intensity plot for comparison of two cone sets to the standard cone set (1.1 mm sampler/0.8 mm skimmer) for dry plasma experimental setup using LA-ICP-MS analysis of NIST 610 glass reference material. Error bars represent  $\pm 1$  standard deviation for mean signal intensity where  $n = 3$ , normalised to standard cone set. Elements arranged in increasing mass-to-charge ratio from left to right. Horizontal lines with asterisks represent a statistically significant difference between the connected data bars at 95% confidence ( $t$ -test). See ESI Fig. S7† for comparison of all orifice sizes studied.

this study, since the area corresponding to the entire droplet was considered during data analysis.

**Ablation of NIST 610 multi-elemental glass reference material (hard particles).** A sample of NIST 610 glass reference material was ablated using a drilling down method to establish possible differences between cone set use and soft or hard particle types. Data collected is displayed in Fig. 4. Similarly to data collection under wet plasma conditions, NIST particle analysis using a dry plasma displays mass bias due to the space charge effect. It is again observed that a complete drop off in signal intensity is recorded using the smallest cone orifices.

As with dry plasma multi-elemental droplet analysis, reducing the orifice of both the sampler and the skimmer cone by 0.1 mm resulted in 7 out of 11 elements displaying a statistically higher background corrected signal intensity for NIST 610 ablation. This trend is predominantly observed for heavier elements and oxides. A higher sensitivity to thorium, uranium and their oxides (compared to the standard set of cones) was also observed when the skimmer cone is kept constant, but the sampler cone is reduced to 0.7 mm (see ESI Fig. S7†). A similar trend in signal-to-noise ratio was observed for the NIST glass as for the gelatine data (see ESI Fig. S8†). All three matrices followed the expected trend of increasing signal-to-noise ratio for elements with higher  $m/z$  values.

## Conclusions

Using the described LA and ICP-MS instrumentation, five sets of ICP sampler and skimmer cones with varying orifice diameters were investigated. Predictably, under wet plasma conditions, the set of cones with the manufacturer recommended orifice diameter consistently produced the highest sensitivity for all

elements measured. Smaller orifices produced a dramatic drop off in sensitivity, plus increased mass bias, due to enhanced space charge effects in the interface region. However, when working with multi-elemental droplets under dry plasma conditions, the effect of reducing cone orifice size was less prominent. Particularly at high masses, an increase in signal intensity was seen when both cone orifice diameters were reduced by 0.1 mm compared to the standard set. This is likely attributable to a combination of lower backgrounds, plus more efficient vacuum readings, which are thought to aid efficient extraction of the ions through the cone orifices. Space charge effects appeared more prominent when hard particles rather than soft were ablated, but a reduction in both cone orifices still had a positive impact on sensitivity for glass analysis, especially for high mass elements.

In recent years, the use of low dispersion LA systems and associated transport accessories has gained popularity, with a variety of manufacturers now producing and selling these devices. Having observed differences in how these systems impact analysis downstream in the mass spectrometer, there is cause for broader investigation into the design of the mass spectrometer interface. It may be the case that the standard design, aimed at solution measurements, is no longer optimum for future laser ablation work. This study supports the hypothesis that devices that remove the need for a Y or T-piece in the LA to ICP transport line may reduce dispersion within the ICP itself and create a narrower package of sample ions at the cone orifice. However, further investigation, including computational modelling is required to confirm this. In this study a variety of elements, spanning a range of chemical properties, were investigated. Future investigations may wish to look at multiple isotopes of each element and determine the



consequences of reducing cone orifices on mass bias for isotope ratio measurements.

## Data availability

Data for this research, including normalised data for both wet and dry plasma modes are available at Loughborough University's repository at: <https://doi.org/10.17028/rd.lboro.27908259.v1>.

## Conflicts of interest

There are no conflicts to declare.

## Acknowledgements

C. A. R. would like to acknowledge the NERC funded CENTA2 DTP, grant NE/S007350/1, for providing funding for a PhD studentship. The authors would like to thank Keith Yendall (Loughborough University) for access to and training on the digital microscope, Tristen Taylor (Elemental Scientific Lasers) for confirmatory data regarding NIST glass ablation and Nathan Westwood (Loughborough University) for advice on data processing and evaluation.

## Notes and references

- 1 J. A. McLean, H. Zhang and A. Montaser, *Anal. Chem.*, 1998, **70**, 1012–1020.
- 2 K. Inagaki, S.-I. Fujii, A. Takatsu and K. Chiba, *J. Anal. At. Spectrom.*, 2011, **26**, 623–630.
- 3 D. P. Myers, G. Li, P. Yang and G. M. Hieftje, *J. Am. Soc. Mass Spectrom.*, 1994, **5**, 1008–1016.
- 4 L. Hendriks, A. Gundlach-Graham, B. Hattendorf and D. Günther, *J. Anal. At. Spectrom.*, 2017, **32**, 548–561.
- 5 S. D. Fernández, N. Sugishama, J. R. Encinar and A. Sanz-Medel, *Anal. Chem.*, 2012, **84**, 5851–5857.
- 6 G. Craig, H. Wehrs, D. G. Bevan, M. Pfeifer, J. Lewis, C. D. Coath, T. Elliott, C. Huang, N. S. Lloyd and J. B. Schwieters, *Anal. Chem.*, 2021, **93**, 10519–10527.
- 7 H. Niu and R. S. Houk, *Spectrochim. Acta, Part B*, 1996, **51**, 779–815.
- 8 M. A. Vaughan and G. Horlick, *Spectrochim. Acta, Part B*, 1990, **45**, 1289–1299.
- 9 N. Taylor and P. B. Farnsworth, *Spectrochim. Acta, Part B*, 2012, **69**, 2–8.
- 10 K. E. Jarvis, P. Mason, T. Platzner and J. G. Williams, *J. Anal. At. Spectrom.*, 1998, **13**, 689–696.
- 11 K. Newman, P. A. Freedman, J. Williams, N. S. Belshaw and A. N. Halliday, *J. Anal. At. Spectrom.*, 2009, **24**, 742–751.
- 12 M. Aghaei, H. Lindner and A. Bogaerts, *J. Anal. At. Spectrom.*, 2013, **28**, 1485–1492.
- 13 M. He, Z. Jin, H. Lu, L. Deng and C. Luo, *Int. J. Mass Spectrom.*, 2016, **408**, 33–37.
- 14 A. Makishima and E. Nakamura, *J. Anal. At. Spectrom.*, 2010, **25**, 1712–1716.
- 15 A. L. Gray, *Analyst*, 1985, **110**, 551–556.
- 16 L. Brunnbauer, V. Zeller, Z. Gajarska, S. Larisegger, S. Schwab, H. Lohninger and A. Limbeck, *Spectrochim. Acta, Part B*, 2023, **207**, 106739.
- 17 C. Arnaudguilhem, M. Larroque, O. Sgarbura, D. Michau, F. Quenet, S. Carrère, B. Bouyssière and S. Mounicou, *Talanta*, 2021, **222**, 121537.
- 18 D. Chew, K. Drost, J. H. Marsh and J. A. Petrus, *Chem. Geol.*, 2021, **559**, 119917.
- 19 P. Ramirez-Hereza, D. Ramos, J. Maroñas, S. A. Balanya and J. Almirall, *Forensic Sci. Int.*, 2023, **349**, 111735.
- 20 A. C. B. C. J. Fernandes, P. Yang, D. Armstrong and R. França, *Talanta*, 2023, **265**, 124909.
- 21 M. Aghaei and A. Bogaerts, *J. Anal. At. Spectrom.*, 2016, **31**, 631–641.
- 22 M. Aghaei, H. Lindner and A. Bogaerts, *Anal. Chem.*, 2016, **88**, 8005–8018.
- 23 H. Lindner and A. Bogaerts, *Spectrochim. Acta, Part B*, 2011, **66**, 421–431.
- 24 D. Günther, H. P. Longerich, S. E. Jackson and L. Forsythe, *Fresenius. J. Anal. Chem.*, 1996, **355**, 771–773.
- 25 C. Latkoczy and D. Günther, *J. Anal. At. Spectrom.*, 2002, **17**, 1264–1270.
- 26 T. He, Q. Ni, Q. Miao and M. Li, *J. Anal. At. Spectrom.*, 2018, **33**, 1021–1030.
- 27 H. A. O. Wang, D. Grolimund, C. Giesen, C. N. Borca, J. R. H. Shaw-Stewart, B. Bodenmiller and D. Gunther, *Anal. Chem.*, 2013, **85**, 10107–10116.
- 28 D. N. Douglas, A. J. Managh, H. J. Reid and B. L. Sharp, *Anal. Chem.*, 2015, **87**, 11285–11294.
- 29 S. J. M. Van Malderen, T. Van Acker and F. Vanhaecke, *Anal. Chem.*, 2020, **92**, 5756–5764.
- 30 S. J. M. Van Malderen, J. T. van Elteren and F. Vanhaecke, *J. Anal. At. Spectrom.*, 2015, **30**, 119–125.
- 31 C. J. Greenhalgh, E. Karekla, G. J. Miles, I. R. Powley, C. Costa, J. de Jesus, M. J. Bailey, C. Pritchard, M. MacFarlane, J. H. Pringle and A. J. Managh, *Anal. Chem.*, 2020, **92**, 9847–9855.
- 32 A. J. Managh and P. Reid, *J. Anal. At. Spectrom.*, 2019, **34**, 1369–1373.

